Metal Nanoparticle Gratings: Influence of Dipolar Particle Interaction on the Plasmon Resonance

B. Lamprecht, G. Schider, R. T. Lechner, H. Ditlbacher, J. R. Krenn, A. Leitner, and F. R. Aussenegg
Institute for Experimental Physics, Karl-Franzens-University Graz and Erwin Schrödinger Institute for Nanoscale Research, Universitätsplatz 5, A-8010 Graz, Austria
(Received 23 December 1999)

We probe the influence of grating effects on plasmon excitations in gold nanoparticles arranged in regular two-dimensional patterns. Samples produced by electron-beam lithography are investigated by femtosecond time-resolved and spectroscopic methods. We find a strong dependence of the plasmon lifetime and resonance wavelength on the grating constant.

PACS numbers: 78.47.+p, 61.46.+w, 73.20.Mf

The interaction of light with metal nanoparticles has been the subject of extensive experimental as well as theoretical research for a long time. Silver and gold nanoparticles with typical sizes of 5–150 nm are of special interest as they can exhibit particularly strong optical extinction in the visible spectral range due to resonantly driven electron plasma oscillations (particle plasmons). Particle plasmons cause local field enhancement and spectral selective light absorption [1]. These properties are of considerable interest in the context of future electronic and optical device applications. Both phenomena are essentially determined by the damping of the particle plasmon, which is manifest in the plasmon decay time τ_{pl} in the time domain and the bandwidth $\Delta\omega$ of the plasmon extinction band in the spectral domain.

For a *single* particle the resonance phenomenon strongly depends on details of the particle shape as well as on the dielectric properties of the particle material and the surrounding medium, respectively. For an *ensemble* of particles, as typically used for experiments, the individual plasmon resonance is additionally influenced by electromagnetic particle interaction. In principle, two types of interaction can be distinguished: near-field coupling and far-field (dipolar) interaction. Near-field coupling is relevant for nearly touching particles due to the short range of the electromagnetic near fields in the order of some tens of nm [2,3]. On the other hand, far-field interaction is mediated by the nanostructures' scattered light fields, which are of dipolar character for nanostructures with sizes much smaller than the light wavelength. Nanoparticles forming an ensemble with particle distances exceeding those allowing near-field coupling are thus interacting via their dipolar fields which interfere to form collective radiation.

This phenomenon has been studied in detail theoretically by Meier, Wokaun, and Liao [4]. For a two-dimensional square grating of metal nanoparticles they found that particularly strong dipolar interaction arises when the light fields, corresponding to a particular grating order, change from evanescent to radiative in character. The critical grating constant which corresponds to the emergence of a new radiation order at a given wavelength is termed d_c (d_{cusp} in [4]), meaning that for $d \leq d_c$ the order is evanescent and for $d \geq d_c$ it is radiating. For the sake of brevity and corresponding to our experimental setup we consider just the case of perpendicular incidence; details on nonperpendicular incidence are given in Ref. [4]. For perpendicular incidence of the exciting light wave and a grating constant d slightly smaller than d_c, the light fields corresponding to a grating order are still evanescent but with the additional property that the local optical fields in the plane of the array become large due to an almost in-phase addition of the scattered light fields of neighboring particles. This results in a modification of the plasmon resonance condition leading to a redshift of the plasmon resonance wavelength [4]. At $d = d_c$ the grating order becomes radiative at a grazing angle. The appearance of a new radiating grating order leads to a sudden increase of the total power radiated by the array, causing enhanced radiation damping of the individual particle plasmons. Because of this additional radiating grating order, plasmon damping is stronger and consequently the plasmon decay time τ_{pl} is smaller for $d \geq d_c$ than for $d \leq d_c$. We thus expect the properties of the individual particle plasmons to be a function of the grating constant defined by the geometrical arrangement of the nanoparticles in the far-field zone of each other. In this Letter we present experimental verifications of this phenomenon which we consider to be of primary importance for the understanding of the physical properties of regularly arranged resonant nanostructures in general.

For sample production we use an electron-beam lithographic method [5], which allows a controlled design of metal nanoparticle gratings. Particle shape and interparticle distance in a square array can be varied independently by this method, enabling us to tailor the optical properties of the single particles independently from the design of the grating parameters. As the investigated particles are well separated (grating constant $\geq$350 nm) the only relevant coupling mechanism is dipolar interaction. This dipolar interaction can be systematically changed by a variation of the grating constant d of the particle grating. As the single particle properties are kept constant in our experiments, a

direct investigation of the influence of the dipolar interaction on the particle plasmon resonance is possible.

Our sample consists of circularly shaped Au nanoparticles arranged in square two-dimensional arrays (side length $\sim 100\ \mu$m) with grating constants varying from 350 to 850 nm. All arrays are deposited on a single indium-tin-oxide coated (mass thickness 3 nm) quartz substrate. The particle height of 14 nm is kept constant for all particles on the substrate. The particle diameter is set equal to 150 nm in order to tune the resulting particle plasmon resonance wavelength to the central wavelength (774 nm) of the fs Ti:sapphire–laser system used in some of the experiments.

For measuring the plasmon decay time τ_{pl} we apply both time and frequency domain methods. To use both methods is reasonable since inhomogeneous absorption band broadening due to nonuniform particle shapes within an investigated particle array cannot be excluded. Therefore we apply a direct fs-time-resolved measurement of the plasmon decay time τ_{pl} [6–9], which, as recently demonstrated [10,11], constitutes a damping determination method that is also applicable in the case of an inhomogeneously broadened plasmon absorption band. The decay time measurement is based on a collinear autocorrelation method [12–14], with 15 fs bandwidth-limited laser pulses [15] for excitation. Third harmonic generation at the particle surface serves as a noninvasive monitor of the local particle plasmon dynamics (third order autocorrelation). The standard deviation of this method is ± 1 fs for resonant particle plasmon excitation. Details on the experimental setup as well as the method in general are described in [16]. Additionally, τ_{pl} is determined from the width of the extinction bands of the particle arrays. Measuring the extinction spectra also yields the position of the plasmon resonance wavelength λ_{res} (wavelength of maximum optical extinction).

In [16] we reported a plasmon decay time of $\tau_{\mathrm{pl}} = 6$ fs for a gold particle array with the specifications described above but with a fixed grating constant of $d = 450$ nm. In this Letter we examine a variation of the grating constant d in order to study the value of τ_{pl} as a function of dipolar interaction (note that shape and size of the individual particles are identical for all arrays). We find the decay time to be strongly dependent on the grating constant d. Figure 1 shows the resulting decay time τ_{pl} for particle arrays with grating constant values d ranging from $d = 350$ nm to $d = 650$ nm. The extinction spectra of these particle arrays are shown in Fig. 2. For comparison, the spectra are normalized to constant particle density in order to obtain comparable extinction for arrays with different grating constants d. We find the extinction spectra to show strongly different bandwidths (FWHM) for the various grating constants ranging from $d = 350$ nm to $d = 850$ nm. Additionally, we find that the peak wavelength λ_{res} varies between 755 and 800 nm as a function of d. We now compare these results with those of the time-resolved measurements. Therefore we extract the value for the decay time τ_{pl} from the bandwidth of the extinction curves using the relation $\Delta\omega\ \tau_{\mathrm{pl}} = 1$. Note that the shape of the extinction curve corresponding to a grating constant of $d = 550$ nm strongly deviates from a Lorentzian, making this consideration problematic in that case. By comparing the resulting τ_{pl} values (solid line in Fig. 3) with those obtained by the time-resolved measurement (Fig. 1), we find an agreement better than 1 fs, which is below the standard deviation of the fs-time-resolved measurement. From this result we conclude that, in our case, inhomogeneous extinction band broadening is negligible. This finding is corroborated by results from the analysis of scanning electron microscope images of our samples, which reveal that the particles are nearly identical in shape with fluctuations of the mean diameter of less than 5%. As the

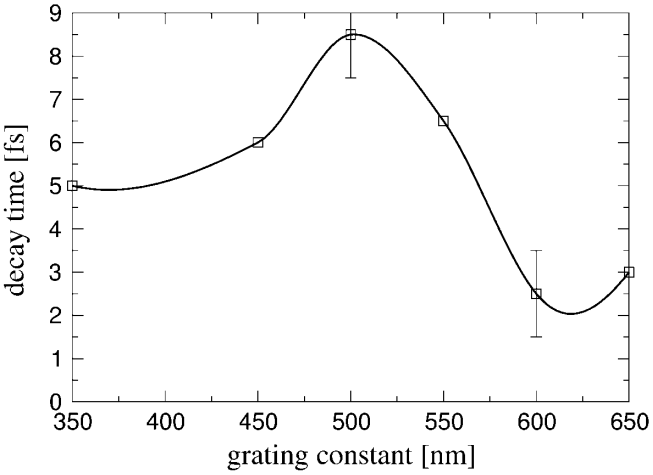

FIG. 1. Plasmon decay time versus grating constant d as obtained from the time-resolved measurement (the solid line is a guide to the eye). Typical error bars are shown for the cases $d = 500$ nm and $d = 600$ nm.

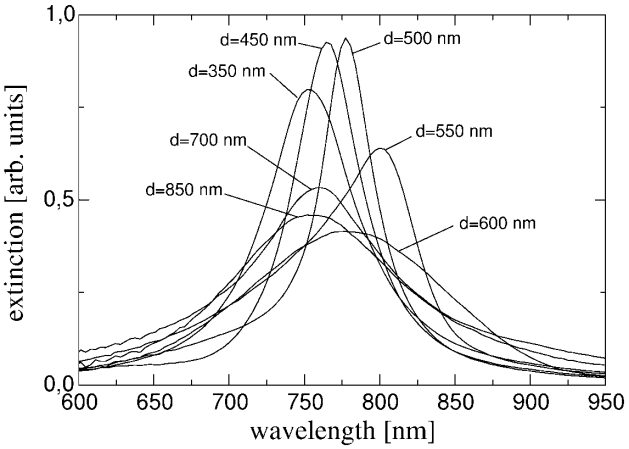

FIG. 2. Extinction spectra for square 2D gratings of Au-nanoparticles (height 14 nm, diameter 150 nm) on an indium-tin-oxide coated quartz substrate (d grating constant).

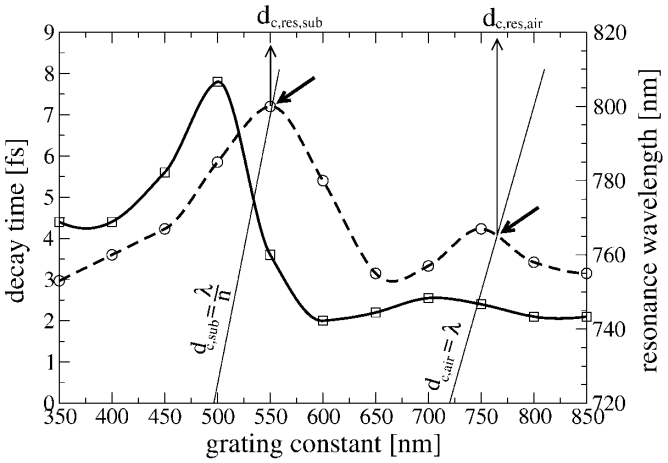

FIG. 3. Solid line: plasmon decay time determined from the FWHM of the extinction spectra (Fig. 2). Dashed line: resonance wavelength (extinction maxima in Fig. 2) versus the grating constant d.

value of the inhomogeneous band broadening is a function of the fluctuations in particle shape, the narrow particle shape distribution causes a negligible inhomogeneous band broadening.

The plasmon decay time τ_{pl}, as extracted from the extinction spectra, and the plasmon resonance wavelength λ_{res} (wavelength of maximum optical extinction in Fig. 2) are plotted versus the grating constant d in Fig. 3. For an interpretation of the dependence of τ_{pl} and the resonance wavelength on the grating constant as found in Fig. 3 we define two specific values of d_c. This is reasonable as our particles are deposited on a substrate (effective refractive index $n = 1.45$), and we therefore obtain two different conditions for the emergence of the first grating order: one for radiation into the substrate ($d_{c,\mathrm{sub}} = \lambda/n$) and one for radiation into the air space ($d_{c,\mathrm{air}} = \lambda$). As the radiated intensity of a single particle becomes maximum for a *resonant* particle plasmon oscillation it is of major interest to consider the special case $\lambda = \lambda_{\mathrm{res}}$, which ranges between 755 and 800 nm for the various particle gratings with different grating constants d (see Figs. 2 and 3). As the resonance wavelength λ_{res} depends on the grating constant d we determine the critical grating constant at resonance of the particle plasmon $d_{c,\mathrm{res}}$ by plotting the lines $d_{c,\mathrm{sub}} = \lambda/n$ and $d_{c,\mathrm{air}} = \lambda$ in Fig. 3. The intersection of these lines with the experimental curve $\lambda_{\mathrm{res}}(d)$ (dashed line) then yields those grating constants $d_{c,\mathrm{res}}$ for which the conditions $d = d_{c,\mathrm{res,sub}}$ or $d = d_{c,\mathrm{res,air}}$ are fulfilled. We find these values at $d_{c,\mathrm{res,sub}} = 550$ nm for radiation in the substrate and $d_{c,\mathrm{res,air}} = 765$ nm for radiation in air (indicated by arrows in Fig. 3). Both values for $d_{c,\mathrm{res}}$ correspond to redshift maxima of the resonance wavelength ($d = 550$ nm and $d = 750$ nm in Fig. 3). We interpret these maxima of redshift as maxima of dipolar interaction at the respective particle distances due to the in-phase addition of the radiation fields of the neighboring particles [4,17].

The decay time τ_{pl} shows the following dependence on the grating constant d. For $d = 500$ nm ($< d_{c,\mathrm{res,sub}}$) where the first grating orders are still evanescent, we measure a maximum decay time of $\tau_{\mathrm{pl}} = 8.5$ fs. This corresponds to a minimum damping of the plasmon oscillation. For $d = 600$ nm ($> d_{c,\mathrm{res,sub}}$) where the fields of the first grating order are radiating in a direction close to the grazing angle, we find a minimum decay time of $\tau_{\mathrm{pl}} = 2.5$ fs, which corresponds to maximum damping. We interpret this dramatically enhanced damping by strongly enhanced radiation damping as being due to radiation of the first grating order into the substrate. For $d = 550$ nm the corresponding extinction curve is asymmetric with respect to the resonance wavelength. This can be understood by the fact that the spectral width of this particular extinction band extends over both low damped (nonradiating) and strongly damped spectral regimes. The observed shape of the extinction curve is in agreement with the results presented in [4]. Qualitatively, the same decay time dependence on the grating constant d also appears at $d_{\mathrm{cusp,air}}$ but with a less pronounced influence on τ_{pl}, due to the already existing strong radiation damping arising from the first order radiating into the substrate.

By investigating random particle distance distributions no significant shift and broadening of the plasmon resonance are found for samples with average interparticle distances ranging from 400 to 1000 nm. This corroborates our finding that shift and broadening of the plasmon resonance are essentially determined by the periodicity of a square array. The dipolar fields of neighboring particles are superimposed with their respective phase shifts, which depend on the distance between the particles.

In conclusion, our results show a dramatic increase in plasmon damping in the transition region from evanescent to radiative fields of the first grating order on the substrate side ($500\ \mathrm{nm} < d < 600\ \mathrm{nm}$). Furthermore we find a strong plasmon resonance wavelength redshift of approximately 50 nm in this transition region. Our experimental findings are in excellent agreement with the theoretical considerations of Meier *et al.* [4]. We explain our results by the 2D periodicity of our particle arrays, which determines the local optical field acting on an individual particle and imposes restrictions on the spatial structure of the scattered far field. Thus the geometrical arrangement of resonant metal nanoparticles in their respective far-field regions crucially influences the individual particle plasmon and thus the plasmon near-field characteristics. This effect should be carefully taken into account when performing optical experiments on samples consisting of ensembles of regularly arranged resonant nanostructures.

The authors thank A. Wokaun for fruitful discussions and for carefully reading the manuscript. Financial support by the Austrian Fond zur Förderung der wissenschaftlichen Forschung, Grant No. P14292-PHY, by the Austrian

Federal Ministry for Science and Traffic, Technology Division, and by the European Union (TMR Project NanoSNOM) is gratefully acknowledged.

[1] U. Kreibig and M. Vollmer, *Optical Properties of Metal Clusters* (Springer, Berlin, 1995).
[2] M. Quinten, A. Leitner, J. R. Krenn, and F. R. Aussenegg, Opt. Lett. **23**, 1331 (1998).
[3] J. C. Weeber *et al.*, Phys. Rev. B **60**, 9061 (1999).
[4] M. Meier, A. Wokaun, and P. F. Liao, J. Opt. Soc. Am. B **2**, 931 (1985).
[5] W. Gotschy, K. Vonmetz, A. Leitner, and F. R. Aussenegg, Appl. Phys. B **63**, 381 (1996).
[6] B. Lamprecht, A. Leitner, and F. Aussenegg, Appl. Phys. B **64**, 269 (1997).
[7] B. Lamprecht, A. Leitner, and F. Aussenegg, Appl. Phys. B **68**, 419 (1999).
[8] J. H. Klein-Wiele, P. Simon, and H. G. Rubahn, Phys. Rev. Lett. **80**, 45 (1998).
[9] M. Simon *et al.*, Chem. Phys. Lett. **296**, 579 (1998).
[10] B. Lamprecht, J. R. Krenn, A. Leitner, and F. R. Aussenegg, Appl. Phys. B **69**, 223 (1999).
[11] T. Vartanyan, M. Simon, and F. Träger, Appl. Phys. B **68**, 425 (1999).
[12] J.-C. M. Diels, J. J. Fontaine, I. C. McMichael, and F. Simoni, Appl. Opt. **24**, 1270 (1985).
[13] C. Spielmann, L. Xu, and F. Krausz, Appl. Opt. **36**, 2523 (1997).
[14] D. Meshulach, Y. Barad, and Y. Silberberg, J. Opt. Soc. Am. B **14**, 2122 (1997).
[15] A. Stingl, C. Spielmann, F. Krausz, and R. Szipcs, Opt. Lett. **19**, 204 (1994).
[16] B. Lamprecht, J. R. Krenn, A. Leitner, and F. R. Aussenegg, Phys. Rev. Lett. **83**, 4421 (1999).
[17] K. T. Carron, W. Fluhr, M. Meier, and A. Wokaun, J. Opt. Soc. Am. B **3**, 430 (1986).